UCRL-JC- 133713
PREPRINT

Fourier Mode Analysis of Slab-Geometry Transport Iterations in Spatially Periodic Media

Michael R. Zika (LLNL)
Edward W. Larsen (University of Michigan)

This paper was prepared for submittal to the
Mathematics & Computation, Reactor Physics and Environmental Analysis in Nuclear Applications
Madrid, Spain
27 - 30 September 1999

April 1, 1999

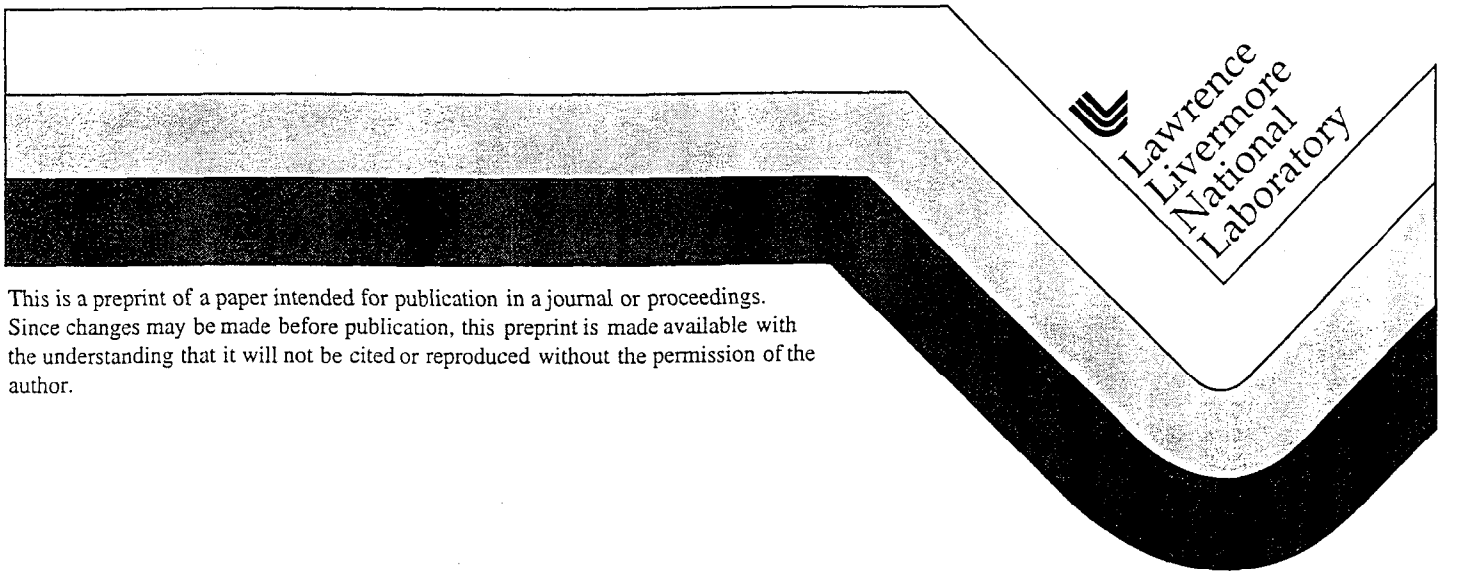

Fourier Mode Analysis of Slab-Geometry Transport Iterations in Spatially Periodic Media

Michael R. Zika
Lawrence Livermore National Laboratory
Livermore, CA (United States)
zika@llnl.gov

Edward W. Larsen
Department Of Nuclear Engineering and Radiological Sciences
University of Michigan
Ann Arbor, MI (United States)
edlarsen@engin.umich.edu

Abstract

We describe a Fourier analysis of the diffusion-synthetic acceleration (DSA) and transport-synthetic acceleration (TSA) iteration schemes for a spatially periodic, but otherwise arbitrarily heterogeneous, medium. Both DSA and TSA converge more slowly in a heterogeneous medium than in a homogeneous medium composed of the volume-averaged scattering ratio. In the limit of a homogeneous medium, our heterogeneous analysis contains eigenvalues of multiplicity two at "resonant" wave numbers. In the presence of material heterogeneities, error modes corresponding to these resonant wave numbers are "excited" more than other error modes. For DSA and TSA, the iteration spectral radius may occur at these resonant wave numbers, in which case the material heterogeneities most strongly affect iterative performance.

1 Introduction

The standard Fourier mode analysis is an indispensable tool when designing acceleration techniques for transport iterations (Larsen, 1984; Adams, 1988; Ramone, 1997); however it requires the assumption of a homogeneous infinite medium. For problems of practical interest, material heterogeneities may significantly impact iterative performance. Recent work has sought to extend the Fourier analysis to include heterogeneous media for spatially discretized and continuous systems; the purpose of this work is to continue this effort.

A Fourier analysis has been applied to the discretized two-dimensional transport operator with heterogeneous material properties (Azmy, 1998; Zika, 1997). The results of these analyses have been difficult to interpret because the heterogeneity effects are inherently coupled to the discretization effects. More recently, a Fourier analysis has been applied to source iteration (SI) for the slab-geometry transport operator in a spatially periodic, heterogeneous medium without spatial discretization (Zika, 1998). However, the transport equation is often not solved using SI, rather an iterative acceleration scheme is applied to obtain more rapid convergence. Two iterative acceleration methods that have been applied to practical problems are diffusion-synthetic acceleration (Larsen, 1982) and transport-synthetic acceleration (Ramone, 1997). In this paper, we apply a Fourier analysis for arbitrarily heterogeneous, spatially periodic media to DSA and TSA.

2 Theory

The Fourier analysis of SI in a spatially periodic medium was presented previously (Zika, 1998). Since both DSA and TSA begin with a single SI step, we first review the theory for source iteration. Then we develop the eigenvalue problems for both DSA and TSA for the case of a spatially periodic, but otherwise arbitrarily heterogeneous, medium. Our approach may be outlined as follows. We begin with equations for the iteration errors in which the material properties retain their spatial dependence. Our Fourier ansatz accounts for this by utilizing a spatially periodic Fourier coefficient. Finally, we manipulate the resulting equations to develop a tractable eigenvalue problem.

2.1 Source Iteration

Consider source iteration for the slab geometry transport equation in a heterogeneous medium. Scaling the spatial variable, x, to a mean free path, the equations for the iteration errors are:

$$\mu\frac{\partial}{\partial x}\hat{\psi}^{(\ell+1/2)}(x,\mu)+\hat{\psi}^{(\ell+1/2)}(x,\mu)=\frac{c(x)}{2}\hat{\phi}^{(\ell)}(x),\quad -\infty\le x\le\infty, \tag{1a}$$

$$\hat{\phi}^{(\ell+1/2)}(x)=\int_{-1}^{1}d\mu'\,\hat{\psi}^{(\ell+1/2)}(x,\mu'). \tag{1b}$$

The notation is standard: $\hat{\psi}^{(\ell)}(x,\mu)$ is the iteration error in the angular flux, $\hat{\phi}^{(\ell)}(x)$ is the iteration error in the scalar flux, $c(x)$ is the scattering ratio, and ℓ is the iteration index. We assume a spatially periodic scattering ratio, $c(x)=c(x+X)$. To proceed with the Fourier analysis, our boundary condition requires that the iteration errors be finite:

$$\lim_{x\to\pm\infty}\hat{\psi}^{(\ell+1)}(x,\mu)<\infty,\quad -1\le\mu\le 1. \tag{2}$$

The source iteration step is completed by updating to the next iterate:

$$\hat{\phi}^{(\ell+1)}(x)=\hat{\phi}^{(\ell+1/2)}(x). \tag{3}$$

Synthetic acceleration schemes (such as DSA and TSA) replace Eq. (3) with an improved iteration update, typically an additive correction (Kopp, 1963).

We now make our Fourier mode ansatz, accounting for the heterogeneity by not seeking a complete separation-of-variables solution (i.e., we assume that the Fourier coefficient is spatially periodic):

$$\hat{\psi}^{(\ell+1/2)}(x,\mu)\equiv\omega^{\ell}a(x,\mu)e^{i\lambda x},\quad \hat{\phi}^{(\ell+1/2)}(x)\equiv\omega^{\ell}A(x)e^{i\lambda x},\quad \hat{\phi}^{(\ell)}(x)\equiv\omega^{\ell}B(x)e^{i\lambda x}. \tag{4}$$

We denote the imaginary number as $i\equiv\sqrt{-1}$, λ is the (real) Fourier parameter, ω is the iteration eigenvalue, and the functions $a(x,\mu)$, $A(x)$ and $B(x)$ are spatially periodic; e.g., $a(x,\mu)=a(x+X,\mu)$. Introducing the Fourier ansatz into Eqs. (1) gives,

$$\left\{\mu\frac{\partial}{\partial x}+(1+i\lambda\mu)\right\}a(x,\mu)=\frac{c(x)}{2}B(x),\quad 0\le x\le X, \tag{5a}$$

$$A(x)=\int_{-1}^{1}d\mu'\,a(x,\mu'). \tag{5b}$$

Since the eigenfunction is spatially periodic, without loss of generality we consider only a single cell, $0 \le x \le X$, with a periodic boundary condition,

$$a(0,\mu) = a(X,\mu), \quad -1 \le \mu \le 1. \tag{6}$$

The iteration update equation, Eq. (3), then becomes,

$$\omega B(x) = A(x). \tag{7}$$

Equations (5) through (7) are the eigenvalue problem for the source iteration eigenvalue, ω. This eigenproblem is a slab geometry transport problem for a complex "angular flux," $a(x,\mu)$, with periodic boundary conditions and a complex removal term. Equations (5) are also the first step in both DSA and TSA.

2.2 Diffusion Synthetic Acceleration

The diffusion synthetic acceleration scheme retains Eqs. (1), but replaces Eq. (3) with,

$$\hat{\phi}^{(\ell+1)}(x) = \hat{\phi}^{(\ell+1/2)}(x) + \hat{f}^{(\ell+1/2)}(x). \tag{8}$$

The iteration errors for the additive correction satisfy a diffusion equation (Larsen, 1984),

$$-\frac{1}{3}\frac{d^2}{dx^2}\hat{f}^{(\ell+1/2)}(x) + \left(1-c(x)\right)\hat{f}^{(\ell+1/2)}(x) = c(x)\left[\hat{\phi}^{(\ell+1/2)}(x) - \hat{\phi}^{(\ell)}(x)\right], \quad -\infty \le x \le \infty. \tag{9}$$

The boundary condition requires that the iteration error in the additive correction be finite as well.

We now augment our Fourier mode ansatz with an analogous expression for the additive corrections

$$\hat{f}^{(\ell+1/2)}(x) \equiv \omega^{\ell} F(x) e^{i\lambda x}, \tag{10}$$

where $F(x)$ is spatially periodic. Introducing our Fourier ansatz retains Eqs. (5) and introduces

$$-\frac{1}{3}\frac{d^2}{dx^2}F(x) - \frac{2}{3}i\lambda\frac{d}{dx}F(x) + \left(1 - c(x) + \frac{\lambda^2}{3}\right)F(x) = c(x)\left[A(x) - B(x)\right], \quad 0 \le x \le X, \tag{11a}$$

$$F(0) = F(X). \tag{11b}$$

The iteration update, Eq. (7) is replaced by,

$$\omega B(x) = A(x) + F(x). \tag{12}$$

By not seeking a complete separation-of-variables solution, we have introduced to the diffusion operator a purely imaginary "advection" term as well as a modified the effective absorption term.

To review, the DSA eigenproblem for the iteration eigenvalue is given by the transport balance equation, Eqs. (5), the equation for the additive corrections, Eqs. (11), and the update equation, Eq. (12). This system is similar to the standard slab-geometry DSA system; however, the solution variables are, in general, complex, and each equation incorporates the wave number, λ.

2.3 Transport Synthetic Acceleration

The transport synthetic acceleration scheme retains Eqs. (1), but replaces Eq. (3) by introducing an additive correction (we use $\hat{g}^{(\ell+1/2)}(x)$ to distinguish between the DSA and TSA corrections):

$$\hat{\phi}^{(\ell+1)}(x) = \hat{\phi}^{(\ell+1/2)}(x) + \hat{g}^{(\ell+1/2)}(x). \tag{13}$$

The iteration errors for the additive correction satisfy a transport equation for which the cross sections have been adjusted to reduce the effective scattering ratio (Ramone, 1997)

$$\mu\frac{\partial}{\partial x}\hat{y}^{(\ell+1/2)}(x,\mu)+\big(1-\beta c(x)\big)\hat{y}^{(\ell+1/2)}(x,\mu)=\frac{(1-\beta)c(x)}{2}\hat{g}^{(\ell+1/2)}(x)$$

$$+\frac{c(x)}{2}\Big[\hat{\phi}^{(\ell+1/2)}(x)-\hat{\phi}^{(\ell)}(x)\Big],\quad -\infty\le x\le\infty, \tag{14a}$$

$$\hat{g}^{(\ell+1/2)}(x)=\int_{-1}^{1}d\mu'\,\hat{y}^{(\ell+1/2)}(x,\mu'). \tag{14b}$$

The TSA parameter, β, satisfies $0\le\beta\le 1$. Once again, the boundary condition requires that the iteration error in the additive correction be bounded.

We retain the Fourier mode ansatz given by Eqs. (5) and add similar expressions for TSA,

$$\hat{g}^{(\ell+1/2)}(x)\equiv\omega^{\ell}G(x)e^{i\lambda x},\quad \hat{y}^{(\ell+1/2)}(x,\mu)\equiv\omega^{\ell}Y(x,\mu)e^{i\lambda x}, \tag{15}$$

where $G(x)$ and $Y(x,\mu)$ are both spatially periodic. Introducing our Fourier ansatz retains Eqs. (5) and introduces equations for the TSA additive corrections,

$$\left\{\mu\frac{\partial}{\partial x}+\big(1-\beta c(x)+i\lambda\mu\big)\right\}Y(x,\mu)=\frac{(1-\beta)c(x)}{2}G(x)+\frac{c(x)}{2}\big[A(x)-B(x)\big],\quad 0\le x\le X, \tag{16a}$$

$$G(x)=\int_{-1}^{1}d\mu'\,Y(x,\mu'), \tag{16b}$$

$$Y(0,\mu)=Y(X,\mu),\quad -1\le\mu\le 1. \tag{16c}$$

The iteration update, Eq. (7) is replaced by,

$$\omega B(x)=A(x)+G(x). \tag{17}$$

Our low-order transport equation, Eq. (16a) now contains a complex removal term.

To review, the TSA eigenproblem for the iteration eigenvalue is given by the transport balance equation, Eqs. (5), the equations for the additive corrections, Eqs. (16) and the update, Eq. (17). This system is similar to the standard slab-geometry TSA system; however, the solution variables are, in general, complex and the system now represents an eigenvalue problem.

2.4 Periodicity Condition

The eigensystems for SI, DSA, and TSA all satisfy the following periodicity condition. If ω is an eigenvalue of one of the eigensystems corresponding to (parameter) λ and eigenfunction $B(x)$, then for any integer n, ω is also an eigenvalue corresponding to $\lambda_n=\lambda-2\pi n/X$ and eigenfunction $B_n(x)=B(x)e^{i2\pi nx/X}$. Thus, without loss of generality, we consider values of the wave number in the range $0\le\lambda\le 2\pi/X$.

This periodicity condition results in the eigenvalue spectrum being composed of a set of eigenvalues based on a "fundamental spectrum," $w(\lambda)$. Consider the spectrum $w(\lambda_0)$, which corresponds to

$n = 0$ (in a homogeneous medium, this is the usual eigenvalue spectrum). According to the periodicity condition, this spectrum is duplicated and translated by $2\pi n/X$ for all integers n. Thus, the *entire* eigenvalue spectrum is the set,

$$\omega(\lambda) = \{w(\lambda_n): n = 0, \pm 1, \pm 2, ...\}. \tag{18}$$

In Fig. 1 we show a subset of $\omega(\lambda)$ for both SI and DSA in a homogeneous medium to illustrate the periodicity condition. This figure shows that a $2\pi/X$ interval is repeated (if all n are displayed). The periodicity condition for TSA is analogous to that of DSA and is not shown.

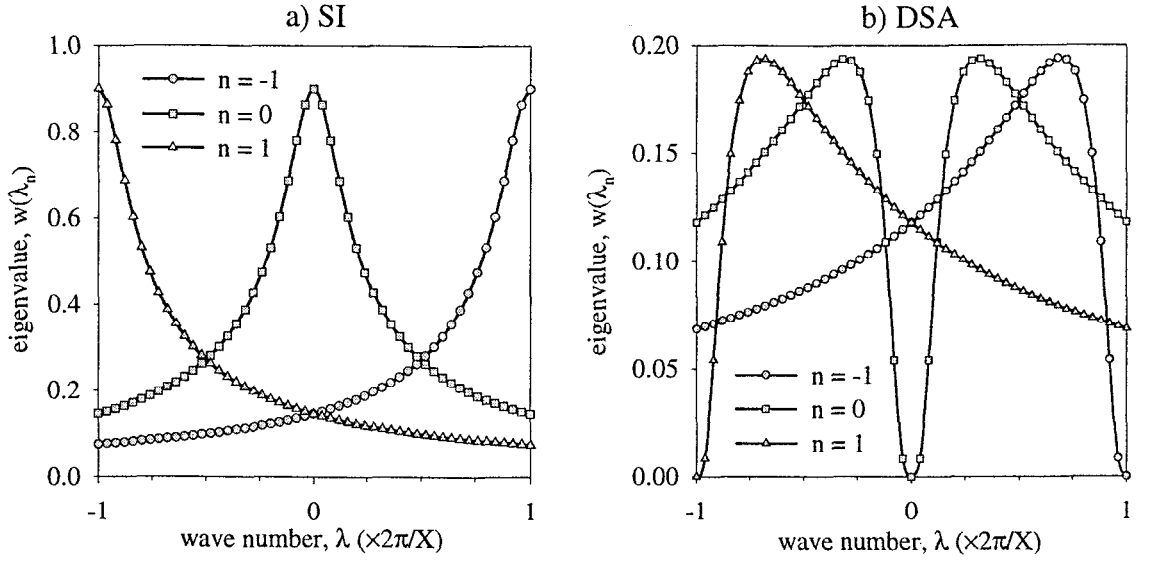

Fig. 1. Periodicity condition of eigenvalue spectra, (a) SI, (b) DSA.

Figure 1 also illustrates the occurrence of eigenvalues of multiplicity two in the spectrum. In the homogeneous case, $w(\lambda)$ is bounded from above by the spectral radius and from below by zero; $w(\lambda)$ is also symmetric about $\lambda = 0$. Under these conditions, $\omega(\lambda)$ will contain an eigenvalue of multiplicity two at $\lambda = \pi/X$, as seen in Fig. 1. The eigenvalue spectrum may contain eigenvalues of multiplicity two at other wave numbers, as can be seen in Fig. 1b. In the heterogeneous case, the presence of such eigenvalues is of particular interest, as discussed below.

3 Results

The standard homogeneous Fourier analysis results in an algebraic expression for the eigenvalue (Larsen, 1984; Ramone, 1997). By contrast, the heterogeneous Fourier analysis yields a system of complex integro-differential equations with periodic boundary conditions. We solve these equations numerically using established discretizations on a well-resolved space- and angle-grid. Our solution algorithm computes only the maximum eigenvalue for a given wave number:

$$W(\lambda) = \sup_n \{w(\lambda_n)\}, \tag{19}$$

where $W(\lambda)$ is a subset of $\omega(\lambda)$. The spectrum $W(\lambda)$ contains the spectral radius of the iteration.

In our calculations, the transport equations, Eqs. (5) and (16) are solved using a diamond-difference spatial discretization and a Gauss-Legendre quadrature set. The diffusion equation, Eqs. (11), is solved using a standard three-point cell-centered spatial discretization; the advection term is differenced using a second-order cell-centered finite difference. Since all calculations are

performed using a fine mesh, the use of an inconsistent diffusion discretization is convergent (Reed, 1971). For the results presented below, the spatial mesh size is never greater than 0.02mfp and an S_{128} discrete-ordinate quadrature set is used. We have performed convergence studies indicating that these resolutions are well-converged in both space and angle.

For our numerical experiments, we have utilized step discontinuities in material properties:

$$c(x)=\begin{cases} c_1, & 0 \le x < X/4 \\ c_2, & X/4 \le x < 3X/4. \\ c_1, & 3X/4 \le x \le X \end{cases} \tag{20}$$

For convenience, we assume $c_2 > c_1$. Thus, the volume-averaged scattering ratio, c_{avg}, is independent of the cell width. Computational experiments indicate that symmetric material heterogeneities such as the one given by Eq. (20) maintain the symmetry of the fundamental spectrum, $w(\lambda)$.

3.1 Source Iteration

In Fig. 2 we show the eigenvalue spectrum of SI for several values of c_1 and c_2. The results for source iteration have been presented previously (Zika, 1998); we reproduce them here to introduce an important feature of the heterogeneous analysis in the context of SI. The eigenspectrum is not uniformly perturbed from the homogeneous spectrum; the error mode corresponding to $\lambda = \pi/X$ is amplified more than other error modes. As stated previously, the homogeneous medium eigenspectrum contains an eigenvalue of multiplicity two at this wave number; we denote the set of such wave numbers as Λ^*. We conjecture that the eigenvalue spectrum bifurcates at the value of each member of Λ^*, resulting in the non-uniform perturbation displayed in Fig. 2 at $\lambda = \pi/X$.

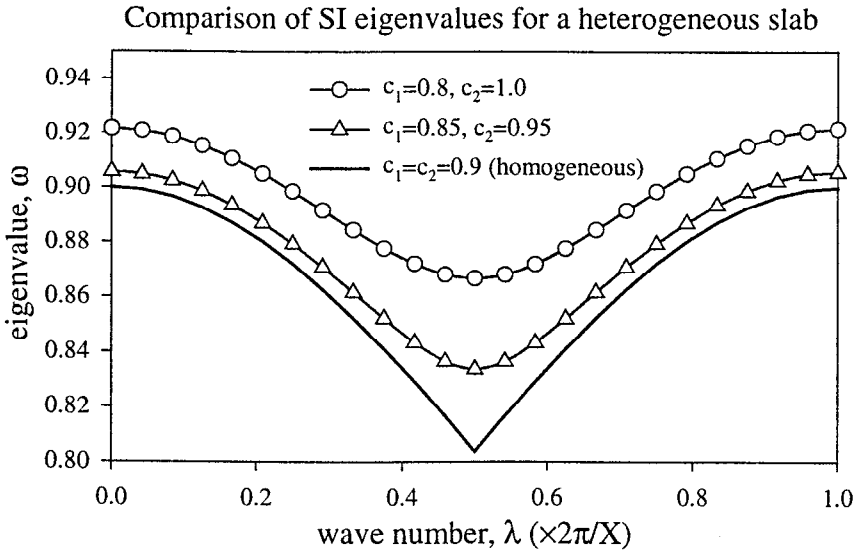

Fig. 2. SI eigenvalues for a heterogeneous slab of two materials (X=5mfp).

The eigenvalue given by the π/X error mode does not result in the spectral radius for SI. The spectral radius corresponds to the $\lambda = 0$ error mode, as in the homogeneous-medium analysis. Therefore, the non-uniform perturbation at $\lambda = \pi/X$ has no effect on the spectral radius.

3.2 Diffusion Synthetic Acceleration

For a homogeneous medium, DSA is designed to be immediately convergent for the $\lambda = 0$ error mode. Unlike SI, the DSA spectral radius in a homogeneous medium is obtained for a non-zero wave number, λ_{max} (a function of the scattering ratio). Based on the results obtained for SI, we expect a similar non-uniform perturbation in the DSA spectrum for homogeneous medium eigenvalues of multiplicity two. Of particular interest are the conditions under which $\lambda_{max} \in \Lambda^*$; i.e., the wave number that yields the homogeneous medium spectral radius corresponds to an eigenvalue of multiplicity two.

We have observed symmetric $w(\lambda)$ for material heterogeneities given by Eq. (20). Given the periodicity condition, we expect that $\lambda = \pi/X$ is a member of Λ^*. From these observations, the "resonant" spatial periodicity of DSA may be computed:

$$X^* = \pi/\lambda_{max}. \tag{21}$$

For a volume-averaged scattering ration, $c_{avg} = 0.9$, the homogeneous medium spectral radius occurs at $\lambda_{max} \cong 2.57 \text{mfp}^{-1}$, resulting in the resonant spatial periodicity $X^* = 1.14\text{mfp}$. In Fig. 3 we show the eigenvalue spectrum of DSA for various values of c_1 and c_2 ($c_{avg} = 0.9$ for all cases) for the resonant spatial periodicity. As expected, the eigenspectrum is not uniformly perturbed from the homogeneous spectrum; the error mode corresponding to $\lambda = \pi/X^*$ is amplified more than other error modes. We note that $\lambda = \{0, 2\pi/X\}$ are also members of Λ^* and display a similar non-uniform perturbation due to the material heterogeneity. However, these values of λ do not affect the spectral radius, as the $\lambda = \pi/X^*$ does.

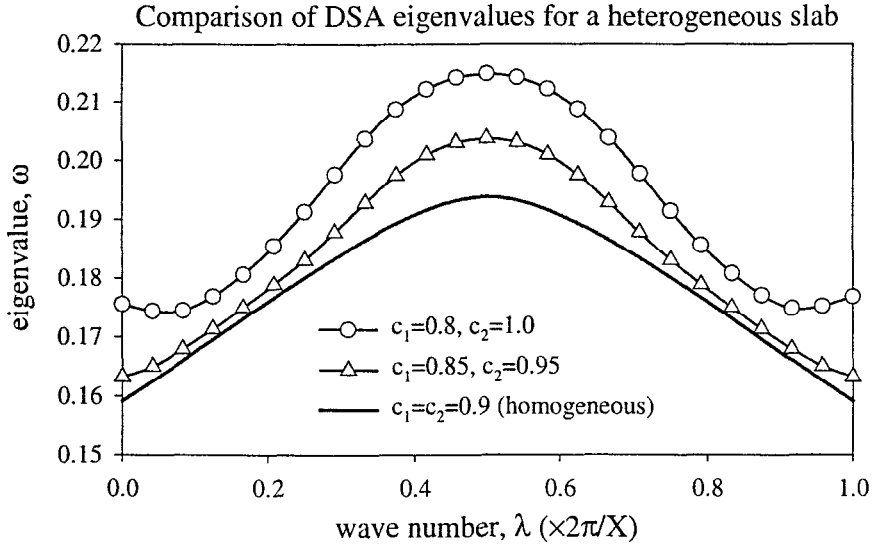

Fig. 3. DSA eigenvalues for a heterogeneous slab of two materials ($X = X^* = 1.14\text{mfp}$).

The spectral radius of DSA corresponds to $\lambda = \pi/X^*$, as designed by our choice of X^*. The effect of the material heterogeneity is not computationally significant; i.e., the resulting spectral radius of 0.215 (compared to 0.194 for the equivalent homogeneous problem) yields rapid iterative convergence. In slab geometry material heterogeneities scale to $0 \le c \le 1$. In multi-dimensional geometries no such scaling exists and material heterogeneities may be arbitrarily large. Thus, in

multi-dimensional geometries, the amplification of such resonant wave numbers may become computationally significant.

In Fig. 4 we show the DSA spectral radius as a function of X, the width of a spatial cell. In the limit of $X \to 0$, the model is an "atomic mix" of materials c_1 and c_2; we expect the spectral radius, ρ, to limit to $\rho(c_{avg})$. In the limit of $X \to \infty$, the model is dominated by the more highly scattering material; we expect the spectral radius to limit to $\rho(c_2)$. We note that the spectral radius is not a monotonically increasing function of X. The resonant spatial periodicity discussed above results in a local maximum in the spectral radius.

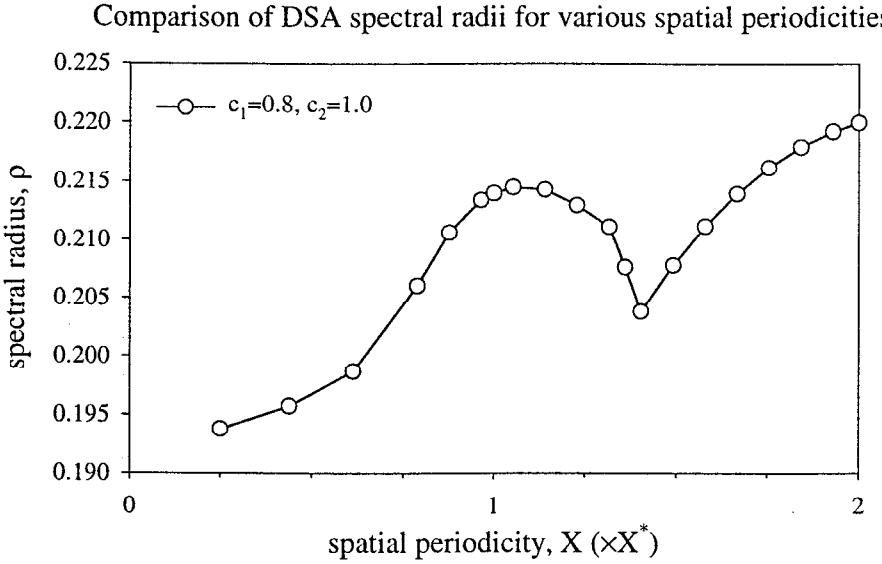

Fig. 4. DSA spectral radii for heterogeneous slabs of two materials.

3.3 Transport Synthetic Acceleration

The TSA scheme is similar to DSA in that it is designed to be immediately convergent for the $\lambda = 0$ error mode. The TSA spectral radius in a homogeneous medium is also obtained for a non-zero wave number, which is a function of both the scattering ratio and the TSA parameter, β. Using the arguments developed for DSA above, we compute the resonant spatial periodicity for TSA. For $c_{avg} = 0.9$ and $\beta = 0.5$, the homogeneous medium spectral radius occurs at $\lambda_{max} \cong 0.641 \text{mfp}^{-1}$, resulting in the resonant spatial periodicity $X^* = 4.9\text{mfp}$. In Fig. 5 we show the eigenvalue spectrum of TSA for various values of c_1 and c_2 for the resonant spatial periodicity. As we observed for DSA, the error mode corresponding to $\lambda = \pi / X^*$ is amplified more than other error modes. The spectral radius of TSA again corresponds to this error mode, as designed by our choice of X^*.

The impact of the spatial periodicity on the spectral radius is not as pronounced for TSA as was observed for DSA. The TSA spectral radius does not contain a significant local maximum as a function of spatial periodicity for the case of $c_1 = 0.8$ and $c_2 = 1.0$.

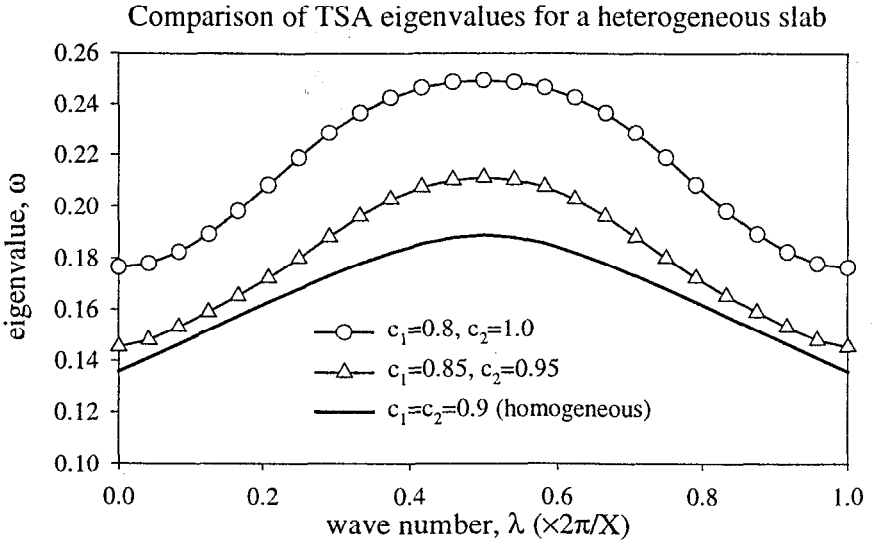

Fig. 5. TSA eigenvalues for a heterogeneous slab of two materials ($X = X^* = 4.9$mfp; $\beta = 0.5$).

3.4 Comparison Against Computational Experiment

To experimentally test the results of our analysis, we consider a thick slab with vacuum boundary conditions. This discretized problem is solved using a four-step DSA algorithm and TSA to obtain an experimental estimate of the spectral radius. In Table I we compare these estimates to the predictions from the Fourier analysis; the spectral radius of the homogenized problem is computed from the volume-averaged scattering ratio. We observe excellent agreement for all material properties tested. The analytic spectral radii are consistently larger than the estimates due to the vacuum boundaries in the computational experiment; the additional loss due to leakage reduces the effective scattering ratio. The values presented in Table I are for the resonant spatial periodicity; we have observed similar agreement between our analysis and computational experiment for all values of the spatial period. Thus, the Fourier analysis provides an accurate prediction of iterative performance.

Table I
Experimental and analytic spectral radii ($X = X^*$)

		spectral radius					
		DSA			TSA (β=0.5)		
c_1	c_2	homogenized	analytic	estimated*	homogenized	analytic	estimated†
0.80	1.00	0.1939	0.2148	0.2140	0.1890	0.2493	0.2472
0.85	0.95	0.1939	0.2038	0.2030	0.1890	0.2114	0.2100
0.81	0.91	0.1939	0.1957	0.1943	0.1890	0.1924	0.1915
0.90	0.90	0.1939	0.1939	0.1930	0.1890	0.1890	0.1881

*100mfp slab, 2.28×10^{-3}mfp mesh width, S_{128}, vacuum boundary conditions, four-step DSA
†245mfp slab, 9.8×10^{-3}mfp mesh width, S_{128}, vacuum boundary conditions, TSA

4 Conclusions

We have extended the Fourier analysis of slab-geometry DSA and TSA to heterogeneous, spatially periodic media. We considered a spatially periodic infinite medium with period X consisting of alternate layers of material with scattering ratios c_1 and c_2. For each acceleration method, our analysis predicts a spectral radius between $\rho(c_1)$ and $\rho(c_2)$, but greater than $\rho(c_{avg})$, where $\rho(c)$ is the

iteration spectral radius of an infinite homogeneous medium with scattering ratio c. Experimental estimates of the spectral radius from an S_N code agree with these theoretical predictions.

The analysis contains a set of wave numbers, Λ^*, that correspond to eigenvalues of multiplicity two in a homogeneous medium. The presence of material heterogeneities excites error modes for these wave numbers more than other error modes. For both DSA and TSA the spatial period, X, may be chosen such that the spectral radius occurs at a wave number in Λ^*. This non-uniform excitation of error modes is not computationally significant in the problems tested (i.e., the acceleration methods remain rapidly convergent). However, in multi-dimensional geometries, material discontinuities may be arbitrarily large (and cannot be largely scaled away, as they can in slab geometry) and the presence of resonant wave numbers may become computationally significant. We plan to investigate extensions of this work to multiple space dimensions and discrete problems, defined on a grid.

Acknowledgments

Work by the first author (MRZ) was performed under the auspices of the U.S. Department of Energy by Lawrence Livermore National Laboratory under contract No. W-7405-Eng-48.

References

[Adams, 1988] Adams, M. L., Boundary Projection Acceleration: A New Approach to Synthetic Acceleration of Transport Calculations, Nucl. Sci. Eng., 100, 177, 1988.

[Azmy, 1998] Azmy, Y. Y., Impossibility of Unconditional Stability and Robustness of Diffusive Acceleration Schemes, Proc. 1998 ANS Topl. Mtg. Radiation Protection and Shielding, Nashville, TN, April 19-23, 1998.

[Kopp, 1963] Kopp, H. J., Synthetic Method Solution of the Transport Equation, Nucl. Sci. Eng., 17, 65, 1963.

[Larsen, 1982] Larsen, E. W., Unconditionally Stable Diffusion-Synthetic Acceleration Methods for the Slab Geometry Discrete Ordinates Equations. Part I: Theory, Nucl. Sci. Eng., 82, 47, 1982.

[Larsen, 1984] Larsen, E. W., Diffusion-Synthetic Acceleration Methods for Discrete-Ordinates Problems, Transport Theory Statist. Phys., 13, 107, 1984.

[Ramone, 1997] Ramone, G. L., Adams, M. L., Nowak, P. F., A Transport-Synthetic Acceleration Method for Transport Iterations, Nucl. Sci. Eng., 125, 257, 1997.

[Reed, 1971] Reed, W. H., The Effectiveness of Acceleration Techniques for Iterative Methods in Transport Theory, Nucl. Sci. Eng., 45, 245, 1971.

[Zika, 1997] Zika, M. R., Iterative Acceleration for Two-Dimensional Long-Characteristics Transport Problems, Ph.D. Dissertation, Texas A&M University, College Station, Texas, 1997.

[Zika, 1998] Zika, M. R., Larsen, E. W., Fourier Mode Analysis of Source Iteration in Spatially Periodic Media, Trans. Am. Nucl. Soc., 79, 137, 1998.